This article has been accepted for publication in a future issue of this journal, but has not been fully edited. Content may change prior to final publication. Citation information: DOI 10.1109/JEDS.2016.2565820, IEEE Journal of the Electron Devices Society

Impact of String Pattern on the Threshold-Voltage Spread of Program-Inhibited Cell in NAND Flash

Yung-Yueh Chiu, Minoru Aoki, Masaru Yano, and Riichiro Shirota, *Senior Member, IEEE*

***Abstract*—An anomalous threshold-voltage (V_t) spread of the program-inhibited cell is investigated for the first time in NAND Flash memory. The program disturb characteristics are studied by applying the program-inhibited stress on the *N*th cell of the unselected bitline (BL) with various string patterns for the 0th to (*N*-1)th cell, using the global self-boosting method (GSB). Distinguishing features of the variance of the number of injected electrons (σ_n^2) into the floating gate are observed. The variance is proportional to the mean value of injected electrons ($\bar{n}$) times 10. The other is proportional to $\bar{n}$ times 20 and occurs only when the (*N*-1)th cell is programmed in a high V_t level and the other cells are in the erased state. A 3-D TCAD simulation reveals that the former case is attributed to Fowler–Nordheim (FN) tunneling from the insufficiently boosting channel, and the latter is explained by hot-electron injection (HCI) owing to the strong lateral electric field between the *N*th and (*N*-1)th cells.**

***Index Terms*—NAND Flash memory, program disturb, Fowler–Nordheim (FN) tunneling, hot-carrier injection (HCI)**

I. Introduction

As NAND Flash memory devices have recently been shrunk to the deca-nanometer scale, various reliability issues, such as threshold-voltage (V_t) distribution spread, associated with electron-injection statistics (EIS), and program disturbance have become serious problems [1]-[5]. In a programing operation of NAND Flash memory, the cells on the selected word-line (WL) are either programmed or program-inhibited depending on the operating schemes. An increase in V_t of the program-inhibited cell is referred to as a program disturbance. To prevent electron injection in program-inhibited cells, the channel potential of the unselected bit-line (BL) is boosted by either the local self-boosting (LSB) method or global self-boosting (GSB) method [6], [7]. The carriers can reportedly be heated by the boosting channel potential and are then injected into the floating-gate (FG). In the LSB method, hot-carrier injection (HCI) is caused mainly by drain-induced barrier lowering (DIBL) that is caused by the large potential difference in the channel [8], [9]. In the GSB method, the HCI effect occurs at the cell that is adjacent to the select-gate (SG) and is caused by gate-induced drain leakage (GIDL) [10]. However, a practical assessment of the impact of the dependence of the HCI effect on the program-inhibited operation is still lacking. Most relevant studies focus on the mean V_t of the program-inhibited cell, and provide no information on its statistics.

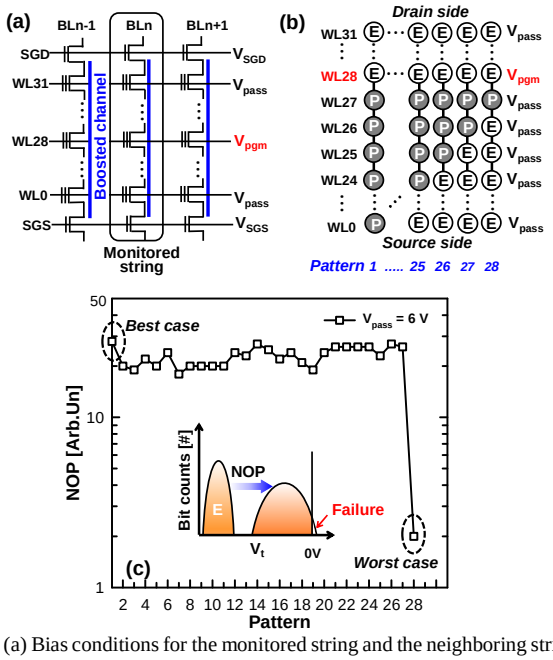

Fig. 1. (a) Bias conditions for the monitored string and the neighboring strings. (b) Various string patterns for program-inhibited test. (c) Experimental comparison of program disturb characteristics based on the string patterns in (b). The inset in Fig. 1(c) reveals that the NOP is evaluated when the cell's tail V_t at +4σquantile shifts to greater than 0V.

This paper elucidates the anomalous V_t spread of program-inhibited cells in a NAND Flash memory array that is caused by the HCI effect. This letter is organized as follows. Section II compares experimental data concerning various string patterns. Section III discusses the electron-injection mechanisms of program-inhibited cells. Section IV presents an analysis of EIS and HCI spread. Finally, conclusions are drawn.

II. Experimental Results

For this experiment, test structures of the 46-nm technology node of NAND Flash memory array were fabricated. A NAND

This work was supported in part by the Winbond Electronics Corporation Japan.

Y. Y. Chiu is with the Department of Electrical and Computer Engineering, Institute of Communications Engineering, National Chiao Tung University, Hsinchu 300, Taiwan. (e-mail: yungyueh.chiu@gmail.com)

M. Aoki and M. Yano are with the Winbond Electronics Corporation Japan, kanagawa 222-0033 (e-mail: maoki@winbond.com; myano@winbond.com).

R. Shirota is with the Department of Electrical and Computer Engineering, Institute of Electrical and Computer Engineering, National Chiao Tung University, Hsinchu 300, Taiwan. (e-mail: riichiro.shirota@gmail.com).

2168-6734 (c) 2016 IEEE. Translations and content mining are permitted for academic research only. Personal use is also permitted, but republication/redistribution requires IEEE permission. See http://www.ieee.org/publications_standards/publications/rights/index.html for more information.

This article has been accepted for publication in a future issue of this journal, but has not been fully edited. Content may change prior to final publication. Citation information: DOI 10.1109/JEDS.2016.2565820, IEEE Journal of the Electron Devices Society

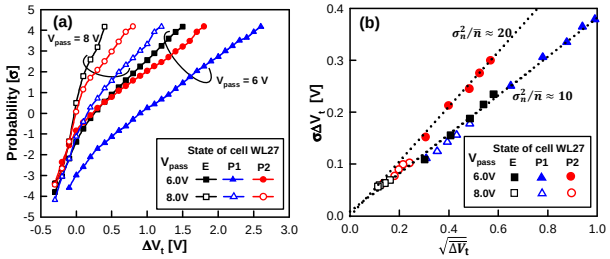

Fig. 2. Measured program disturb characteristics for worst pattern "28" in Fig. 1. (a) Program disturbance of target cell (when WL27 state = E (squares); when WL27 = P1 (triangles); when WL27 = P2 (circles)). (b) Measured $\sigma\Delta V_t$ as a function of $\overline{\Delta V_t}$.

cell string is composed 32 unit cells, a source select line transistor and a drain select line transistor. In the program-inhibited test, the channel potential of either the monitored string or neighboring strings is boosted by GSB method, as shown in Fig. 1(a). For the monitored string, specific patterns were obtained by selective programming of the cells, as presented in Fig. 1(b), in which "E" denotes the erased state of the cell and "P" denotes the programmed state (V_t = 3 V). Furthermore, cells on the neighboring strings are all in E state. Then, the program-inhibited pulse was repeatedly applied to the cell connected to WL28 (cell WL28). Here, V_{pgm} (20V) and V_{pass} (6 V) are applied to control-gate (CG) and pass cells, respectively. Since significant cell-to-cell differences exist, a statistical method in which approximately 2×10^4 cells were monitored in each pattern was utilized. Fig. 1(c) shows the string pattern dependence of program disturbance. The number of allowable programming cycles (NOP) was evaluated when the target cell's V_t at the $+4\sigma$ shifted to more than 0V, as shown in the inset of Fig. 1(c). The program disturbance of the pattern 28 is significantly worse than that of other patterns.

To clarity this result, the V_t of all program-inhibited cells in WL28 was initially set to 0.5V and their V_t shifts were monitored. Then, the V_t shift (ΔV_t) spread regarding the "28" pattern whose characteristics are greatly affected by the state of cell WL27 (-3 V, 1.5 V, and 3V, denoted states E, P1, and P2, respectively) were monitored and presented in Fig. 2(a). The standard deviations ($\sigma\Delta V_t$) of ΔV_t spread under program-inhibited stress was proportional to the square-root of its average value ($\overline{\Delta V_t}$), as presented in Fig. 2(b). The V_t spread is strictly related to the standard deviation of the number of injected electrons n, as follows.

$$\sigma\Delta V_t = \frac{q}{C_{pp}}\sqrt{\sigma_n^2} \tag{1}$$

where q is the electronic charge and C_{pp} is the CG-to-FG capacitance. The value of $\overline{\Delta V_t}$ is obtained with the classical formula of memory devices $\overline{\Delta V_t} = q\bar{n}/C_{pp}$. Accordingly, the relation between $\sigma\Delta V_t$ and $\overline{\Delta V_t}$ is given by

$$\sigma\Delta V_t = \sqrt{\frac{\sigma_n^2}{\bar{n}} \cdot \frac{q}{C_{pp}} \cdot \overline{\Delta V_t}} \tag{2}$$

where $\bar{n}$ is the mean value of n. Accordingly, the $\sigma_n^2/\bar{n}$ ratio

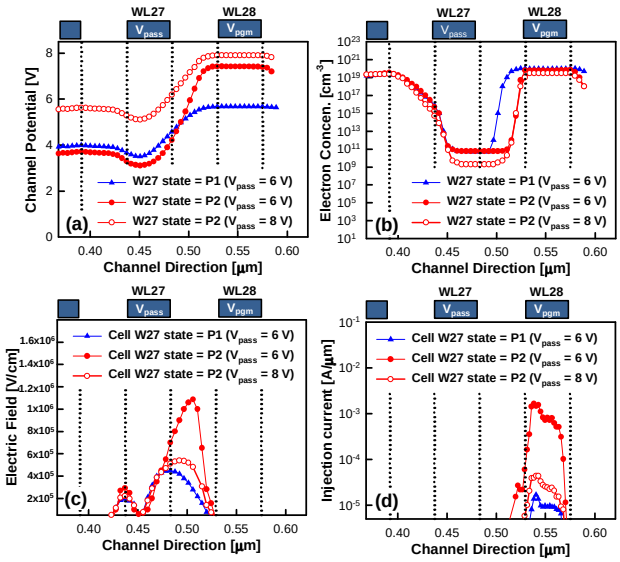

Fig. 3. Simulated (a) self-boosting channel potential, (b) electron concentration, (c) electric field, and (d) hot-electron injection (HCI) current of cell WL27 in the P1 and P2 states.

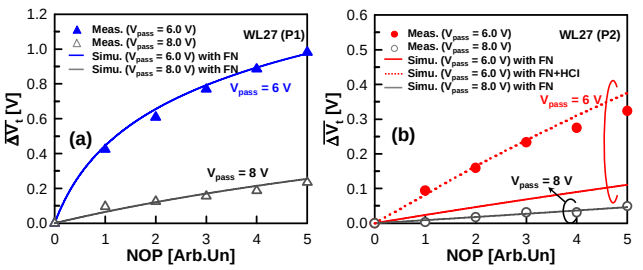

Fig. 4. Measured (symbols) and simulated (lines) $\overline{\Delta V_t}$ of program-inhibited cell with cell W27 in (a) P1 and (b) P2 state. Simulations have been performed including FN tunneling or HCI effect. Dotted lines represent simulated results obtained by including contribution of HCI to $\overline{\Delta V_t}$.

remains constant as the cell's V_t varies. The $\sigma_n^2/\bar{n}$ ratio in all cases is approximately 10, except when cell WL27 is in the P2 state and V_{pass} is 6V, when the ratio equals 20.

III. Simulation Results and Disscussinos

To investigate the origin of the EIS, a comprehensive 3-D TCAD simulation that is based on the fabrication of 46-nm NAND Flash devices is performed. The channel potential, electric field, electron concentration, and HCI current of cell WL27 in the P1 are compared with those in the P2 state, as shown in Fig. 3. The figure reveals that the V_t level of cell WL27 significantly affects on the potential of target cell. The boosting potential of cell WL28 increases with the V_t of cell WL27 because the potential barrier of cell WL27 suppresses electrons to drift or diffuse to cell WL28. In the case of cell WL27 in state P1 at $V_{pass} = 6\,V$, a locally strong electric field is therefore established by the potential difference between the WL27 and WL28 space region. The channel electrons are accelerated by the high electric field and the lucky electrons [11] are thus injected into the FG of cell WL28.

To verify the dependence V_t of cell WL27 on program disturb characteristics, the measured $\overline{\Delta V_t}$ transients of the target cell are compared with the simulated values for the cell WL27

2168-6734 (c) 2016 IEEE. Translations and content mining are permitted for academic research only. Personal use is also permitted, but republication/redistribution requires IEEE permission. See http://www.ieee.org/publications_standards/publications/rights/index.html for more information.

This article has been accepted for publication in a future issue of this journal, but has not been fully edited. Content may change prior to final publication. Citation information: DOI 10.1109/JEDS.2016.2565820, IEEE Journal of the Electron Devices Society

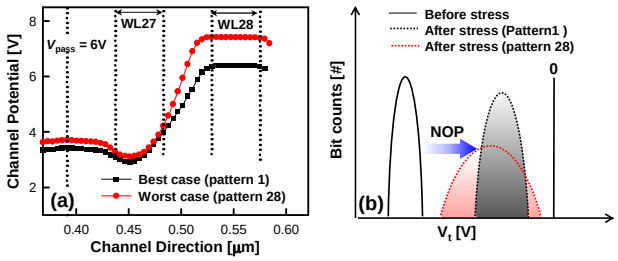

Fig. 5. (a) Simulated boosting potential and (b) V_t distribution of the worst and best case in Fig. 1(c).

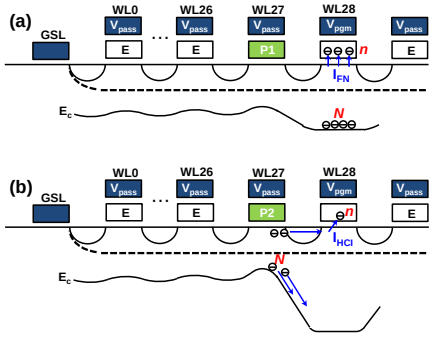

Fig. 6. Schematics for the electron-injection events in program-inhibited string of cell W27 in (a) P1 and (b) P2 states.

in P1 and P2 states, as presented in Fig. 4. The simulation involves basic FN tunneling and the HCI effect that is associated with the boosting channel. The simulations agree closely with experimental data and reveal the mechanisms that dominate the program disturb characteristics. In the case of cell W27 in P1 state [Fig. 4(a)], the program disturbance is mainly dominated by the Fowler–Nordheim (FN) tunneling. In the case of cell W27 in P2 state [Fig. 4(b)], the simulations without HCI component does not match the experimental data when $V_{pass} = 6$ V. However, the HCI effect becomes negligible as the V_{pass} level increases owing to the decrease in the potential difference between the WL27 and WL28. Comparing the results in Fig. 2(b) and Fig. 4 reveals that the $\sigma_n^2/\bar{n}$ ratios of 10 and 20 correspond to FN- and HCI-induced program disturbance. Note that the experimental results show that the V_{pass} level should be kept in the range of 8 to 10 V to suppress the V_{pass} and HCI-induced disturbance.

To elucidate the dependence of string pattern on the program disturbance, the boosting potential of the worst and best case in Fig. 1(c) are shown in Fig. 5(a). However, it is clearly seen that the boosting potential in the best case is lower than that in the worst case. This can be explained as follows: In the best case, the program disturbance is mainly caused by FN tunneling. The V_t distribution tail of the best case is more negative than that of the worst pattern because the EIS is smaller compared with the HCI spread, as depicted in Fig. 5(b). Furthermore, if the selected cell is programed to have V_t higher than 3V (P3 state), the boosting potential transition (ΔV_{ch}) in the best case can be estimated as [1]

$$\Delta V_{ch} = -\frac{28}{32}\gamma\left[V_t(P3) - V_t(P2)\right] \tag{3}$$

where γ is the gate coupling ratio. As a result, the FN-induced program disturbance becomes more serious. In the worst case, as the V_t of cell WL27 increases, the potential difference between the WL27 and WL28 increases. Consequently, the enhanced electric field results in a larger ΔV_t.

IV. Statistics Concerning Injection Electrons

This section focuses on the EIS and HCI spread. In the case of FN-induced program disturbance, N is the number of channel electrons in cell WL28 that can be injected into FG, as shown in Fig. 6(a). In the case of HCI-induced program disturbance, N is the number of electrons that are accelerated by the strong lateral electric field, as shown in Fig. 6 (b). Since the $\sigma_n^2/\bar{n}$ ratio remains constant as time escape, the probability function of injection events $b(n, N)$ can be treated as mutually independent and their statistics follow a binominal distribution, described by

$$b(n,N) = \binom{N}{n} P(t)^n \left[1 - P(t)\right]^{N-n} \tag{4}$$

where $P(t)$ is the probability of the injected electrons at time t. Therefore, the resulting $\bar{n}$ and the corresponding σ_n^2 can be expressed as

$$\bar{n} = N \cdot P(t) \tag{5}$$

$$\sigma_n^2 = \bar{n}\left[1 - P(t)\right] \tag{6}$$

To take into account the statistical dispersion of N, (5) and (6) can be written as (see calculation in Appendix)

$$\bar{n} = \bar{N} \cdot P(t) \tag{7}$$

$$\sigma_n^2 = \bar{n} + \left(\sigma_N^2 - \bar{N}\right) P(t)^2 \tag{8}$$

where $\bar{N}$ and σ_N^2 are the mean and variance of N, respectively. By comparing the results of σ_n^2 obtained from measurements, it reveals that σ_N^2 is significantly larger than $\bar{N}$. During program-inhibited stress, the dispersion of N is strictly related to the fluctuation of boosting potential owing to the variation of the electrons flow from the source side cells to cell WL28. This effect is obvious when many WLs are boosted together. Additionally, in the case of HCI-induced program disturbance, cell WL27 forms a barrier for electrons in the source side cells to drift to cell WL28, which may widen the dispersion of N.

The above results suggest that there are two methods for suppressing the program disturbance. One is to increase the boosting potential and hence reducing $P(t)$, e.g., source/drain junction engineering [12]. The other is to decrease N at the program-inhibited cell, e.g., programming disturb-free scheme (PDFS) [4].

V. Conclusion

A detailed investigation of the V_t spread of program-inhibited cell due to FN tunneling and HCI effect has been presented. Both the previous leakage currents result into a broadening of the V_t spread, but the statistical dispersion of

2168-6734 (c) 2016 IEEE. Translations and content mining are permitted for academic research only. Personal use is also permitted, but republication/redistribution requires IEEE permission. See http://www.ieee.org/publications_standards/publications/rights/index.html for more information.

This article has been accepted for publication in a future issue of this journal, but has not been fully edited. Content may change prior to final publication. Citation information: DOI 10.1109/JEDS.2016.2565820, IEEE Journal of the Electron Devices Society

injected electrons was greater for the HCI-induced than for the FN-induced program disturbance. Therefore, the HCI effect that is caused by the NAND string pattern is a new issue that needs to be managed in a program-inhibited operation.

VI. Acknowledgment

The authors would like to thank all of the members of the NAND Flash development team in Winbond Electronics Corporation for discussions and support.

Appendix

The $\bar{n}$ can be express as

$$\begin{aligned}\bar{n} &= \sum_{n=0}^{\infty} n \cdot b(n) = \sum_{n=0}^{\infty} n \sum_{N=0}^{\infty} b(n,N) \cdot b(N) \\ &= \sum_{N=0}^{\infty} b(N) \cdot \sum_{n=0}^{N} nb(n,N) = \sum_{N=0}^{\infty} b(N) \cdot NP(t) \\ &= \bar{N} \cdot P(t)\end{aligned}$$

where the $b(n)$ and $b(N)$ are the probability density function of n and N, respectively. The σ_n^2 can be calculated as

$$\begin{aligned}\sigma_n^2 &= \sum_{n=0}^{\infty} \left(n-\bar{n}\right)^2 \cdot b(n) = \sum_{n=0}^{\infty} \left(n-\bar{n}\right)^2 \sum_{N=0}^{\infty} b(n,N) \cdot b(N) \\ &= \sum_{N=0}^{\infty} b(N) \cdot \sum_{n=0}^{N} \left(n^2 - 2n\bar{n} + \bar{n}^2\right) \cdot b(n,N) \\ &= \sum_{N=0}^{\infty} b(N) \cdot \Big[NP(t)\left(1-P(t)\right) + N^2 P(t)^2 \\ &\qquad -2N\bar{N}P(t)^2 + \bar{N}^2 P(t)^2 \Big] \\ &= \bar{n} + \left(\sigma_N^2 - \bar{N}\right) P(t)^2 .\end{aligned}$$

References

[1] S. Satoh, H. Hagiwara, T. Tanzawa, K. Takeuchi, and R. Shirota, "A novel isolation-scaling technology for NAND EEPROMs with the minimized program disturbance," in *IEDM Tech. Dig.*, 1997, pp. 291–294.

[2] C. Monzio Compagnoni, C. Miccoli, A. L. Lacaita, A. Marmiroli, A. S. Spinelli, and A. Visconti, "Impact of control-gate and floating-gate design on the electron-injection spread of decananometer NAND Flash memories," *IEEE Electron Device Lett.*, vol. 31, no. 11, pp. 1196–1198, Nov. 2010.

[3] R. Shirota, Y. Sakamoto, H.-M. Hsueh, J.-M. Jaw, W.-C. Chao, C.-M. Chao, S.-F. Yang, and H. Arakawa, "Analysis of the correlation between the programmed threshold-voltage distribution spread of NAND Flash memory devices and floating-gate impurity concentration," *IEEE Trans. Electron Devices*, vol. 58, no. 11, pp. 3712–3919, Nov. 2011.

[4] R. Shirota, C.-H. Huang, S. Nagai, Y. Sakamoto, F.-H. Li, N. Mitiukhina, and H. Arakawa, "A new programming scheme for the improvement of program disturb characteristics in scaled NAND flash memory," *IEEE Trans. Electron Devices*, vol. 59, no. 10, pp. 2767 - 2773, Oct. 2012.

[5] A. Torsi, Y. Zhao, H. Liu, T. Tanzawa, A. Goda, P. Kalavade, and K. Parat, "A program disturb model and channel leakage current study for sub-20 nm NAND Flash cells," *IEEE Trans. Electron Devices*, vol. 58, no. 1, pp. 11–15, Jan. 2011.

[6] K.-D. Suh, B.-H. Suh, Y.-H. Lim, J.-K. Kim, Y.-J. Choi, Y.-N. Koh, S.-S. Lee, S.-C. Kwon, B.-S. Choi, J.-S. Yum, J.-H. Choi, J.-R. Kim, and H.-K. Lim, "A 3.3 V 32 Mb NAND Flash memory with incremental step pulse programming scheme," in *ISSCC Tech. Dig.*, 1995, pp. 128–129.

[7] D. Oh, C. Lee, S. Lee, T.-K. Kim, J. Song, and J. Choi, "A new self-boosting phenomenon by source/drain depletion cut-off in NAND flash memory," in *Proc. Non-Volatile Semicond. Memory Workshop*, 2007, pp. 39–41.

[8] M. Kang, W. Hahn, I.-H. Park, J. Park, Y. Song, H. Lee, C. Eun, S. Ju, K. Choi, Y. Lim, S. Jang, S. Cho, C. Eun, S. Ju, K. Choi, Y. Lim, S. Jang, S. Cho, B.-G. Park, and H. Shin, "DIBL-Induced program disturb characteristics in 32-nm NAND flash memory array," *IEEE Trans. Electron Devices*, vol. 58, no. 10, pp. 3626–3629, Oct. 2011.

[9] D.-Y. Oh, S. Lee, C. Lee, J. Song, W. Lee, and J. Choi, "Program disturb phenomenon by DIBL in MLC NAND Flash device," in *Proc. IEEE NVSMW*, May 2008, pp. 5–7.

[10] J.-D. Lee, C.-K. Lee, M.-W. Lee, H.-S. Kim, K.-C. Park, and W.-S. Lee, "A new programming disturbance phenomenon in NAND Flash memory by source/drain hot-electron generated by GIDL current," in *Proc. IEEE NVSMW*, Feb. 2006, pp. 31–33.

[11] S. Tam, P.-K. Ko, and C. Hu, "Lucky-electron model of channel hot-electron injection in MOSFETs," *IEEE Trans. Electron Devices*, vol. 31, no. 9, pp. 1116–1125, Sep. 1984.

[12] S. Satoh, T. Nakamura, K. Shimizu, K. Takeuchi, H. Iizuka, S. Aritome, and R. Shirota, "A novel gate-offset NAND cell (GOC-NAND) technology suitable for high-density and low-voltage-operation flash memories," in I*EDM Tech. Dig.*, 1999, pp. 271–274.

Yung-Yueh Chiu received M.S. degree from National Chiao-Tung University, Hsinchu, Taiwan, in 2012, where he is currently pursuing the Ph.D. degree with the Institute of Communications Engineering. His research interests include modeling and simulation of NAND Flash memory.

Minoru Aoki, photograph and biography not available at the time of publication.

Masaru Yano, photograph and biography not available at the time of publication.

Riichiro Shirota (M'12-SM'12) received the B.S., M.S., and Ph.D. degrees in physics in 1977, 1979, and 1982, respectively, all from Nagoya University, Nagoya, Japan.

He became a Professor with National Tsing Hua University, Hsinchu, Taiwan, in 2006 and has been a Professor with National Chiao Tung University, Hsinchu, since 2010. His current research interests are the modeling of Flash memory cell.

2168-6734 (c) 2016 IEEE. Translations and content mining are permitted for academic research only. Personal use is also permitted, but republication/redistribution requires IEEE permission. See http://www.ieee.org/publications_standards/publications/rights/index.html for more information.